

Single-Cell Transcriptomics Identifies a Prominent Role for the MIF-CD74 Axis in Myasthenia Gravis Thymus

Paula Terroba-Navajas,¹ I-Na Lu,¹ Isaak Quast,² Michael Heming,¹ Christian W. Keller,^{1,3} Lennard Ostendorf,^{4,5,6} Anja Erika Hauser,^{7,8} Ronja Mothes,^{5,9} Helena Radbruch,⁹ Frauke Stascheit,¹⁰ Andreas Georg Otto Meisel,¹⁰ Heinz Wiendl,^{1,3} Gerd Meyer Zu Hörste,¹ Nick Willcox,¹¹ and Jan D. Lünemann¹

Correspondence
Prof. Lünemann
jan.luenemann@ukmuenster.de

Neurol Neuroimmunol Neuroinflamm 2025;12:e200384. doi:10.1212/NXI.0000000000200384

Abstract

Background and Objectives

Myasthenia gravis (MG) is an autoimmune disease most frequently caused by autoantibodies (auto-Abs) against the acetylcholine receptor (AChR) located at the neuromuscular junction. Thymic follicular hyperplasia is present in most of the patients with early-onset AChR-Ab⁺ MG (EOMG), but its cellular and molecular drivers and development remain poorly understood.

Methods

We constructed a single cell-based transcriptional profile of lymphoid cell types in thymi from 11 immunotherapy-naïve patients with EOMG. Multiplex histology and ELISA were used to determine migration inhibitory factor (MIF) levels.

Results

Within EOMG thymi, we consistently observed 6 distinct clusters of B-cell populations maturing toward germinal center (GC)-associated and Ab-secreting cells, featuring prominent GC activity, as indicated by substantial clonal expansions and cycling B-cell subsets. Cell-cell interactome predictions identified strong interactions between T cells and GC-associated and memory B cells, dominated by B-cell prosurvival signaling through the MIF-CD74 axis. Multiplex histology confirmed abundant expression of CD74 in MG thymic B cells. Circulating MIF levels in EOMG correlated with higher disease severity as assessed by Myasthenia Gravis Foundation of America status.

Discussion

Our data not only illustrate and define hyperplastic thymic niches in MG as favorable environments for pathogenic B-cell proliferation, maturation, and persistence but also suggest that the MIF-CD74 axis should be investigated for potential novel therapeutic targeting in EOMG.

Introduction

The localized or general muscle weakness in most patients with myasthenia gravis (MG) is mediated by auto-Abs exclusively specific for the native conformation of the acetylcholine

¹Department of Neurology with Institute of Translational Neurology, University Hospital Münster, Germany; ²Department of Immunology, Monash University, Melbourne, VIC, Australia; ³Department of Neurology and Neurophysiology, University Hospital Freiburg, Germany; ⁴Department of Nephrology and Medical Intensive Care, Charite Universitätsmedizin Berlin, Corporate Member of Freie Universität Berlin, Humboldt-Universität zu Berlin, and Berlin Institute of Health, Germany; ⁵Deutsches Rheuma-Forschungszentrum (DRFZ), an Institute of the Leibniz Association, Berlin, Germany; ⁶BIH Biomedical Innovation Academy, BIH Charité Junior Clinician Scientist Program, Berlin Institute of Health at Charité-Universitätsmedizin Berlin, Germany; ⁷Department of Rheumatology and Clinical Immunology, Charite Universitätsmedizin Berlin, Corporate Member of Freie Universität Berlin, Humboldt-Universität zu Berlin, and Berlin Institute of Health, Germany; ⁸Immune Dynamics, Deutsches Rheuma-Forschungszentrum (DRFZ), a Leibniz Institute, Berlin, Germany; ⁹Department of Neuropathology, Charite Universitätsmedizin Berlin, Corporate Member of Freie Universität Berlin, Humboldt-Universität zu Berlin, and Berlin Institute of Health, Germany; ¹⁰Department of Neurology with Experimental Neurology, Neuroscience Clinical Research Center, Charite Universitätsmedizin Berlin, Corporate Member of Freie Universität Berlin, Humboldt-Universität zu Berlin, and Berlin Institute of Health, Germany; and ¹¹Departments of Clinical Neurosciences, Royal Free Hospital, London Until 1988, Then Weatherall Institute of Molecular Medicine, University of Oxford, United Kingdom.

The Article Processing Charge was funded by the authors.

This is an open access article distributed under the terms of the Creative Commons Attribution-Non Commercial-No Derivatives License 4.0 (CCBY-NC-ND), where it is permissible to download and share the work provided it is properly cited. The work cannot be changed in any way or used commercially without permission from the journal.

Copyright © 2025 The Author(s). Published by Wolters Kluwer Health, Inc. on behalf of the American Academy of Neurology.

e200384(1)

MORE ONLINE

Supplementary Material

Glossary

AChR = against the acetylcholine receptor; **CLL** = chronic lymphocytic leukemia; **CSR** = Ig class switch DNA recombination; **DC** = dendritic cell; **DFG** = Deutsche Forschungsgemeinschaft; **EOMG** = early-onset AChR-Ab+ MG; **GC** = germinal center; **HLA** = human leukocyte antigen; **MG** = myasthenia gravis; **MGFA** = Myasthenia Gravis Foundation of America; **MIF** = migration inhibitory factor; **PC** = plasmablast/plasma cell; **QMG** = quantitative MG disease score; **RTX** = rituximab; **SHM** = somatic hypermutation; **TFH** = thymic follicular hyperplasia.

receptor (AChR), uncommonly instead against other functionally related surface molecules on the postsynaptic motor endplate.¹ However, the mechanisms leading to the selective production of these auto-Abs in MG are poorly understood.

Thymic follicular hyperplasia (TFH) is prominent in most patients with early-onset MG (EOMG),¹⁻⁷ who represent approximately 30% of all patients with MG.¹ Characterized by lymph node-like infiltrates with T-cell areas and germinal centers (GCs) in medullary perivascular spaces,¹⁻⁷ TFH occurs, but less frequently, in other autoimmune diseases such as lupus erythematosus, rheumatoid arthritis, or myelin oligodendrocyte glycoprotein Ab-associated disease, among many others.⁸⁻¹¹ The only cells outside muscle to express native AChR are the rare muscle-like medullary thymic myoid cells, which have long been implicated in EOMG pathogenesis.^{2,6,12} Notably, the cell types required to initiate and maintain auto-Ab responses to AChR are present in the EOMG thymus. Indeed, B-lineage cells there spontaneously produce these auto-Abs,^{2,4-7,13} and thymectomy often results in significant clinical improvement.^{1,12,14,15} In this study, by constructing a detailed atlas of EOMG thymic leukocytes using single-cell RNA sequencing combined with multiplex histology, we identify molecular and cellular underpinnings of pathologic B-lineage cell maturation, survival, and persistence in the EOMG thymus, highlighting an unexpected role for the MIF-CD74 axis.

Methods

Patients

We recruited 12 immunotherapy-naïve and corticosteroid-naïve patients with AChR-Ab⁺ EOMG from the National Hospital for Nervous Diseases, London, United Kingdom, and Oxford University Hospitals, United Kingdom (eTable 1), for scRNA-seq analysis; 32 MG serum samples for MIF ELISA analysis (eTable 2) and 3 others from the Charité University Hospital Berlin for multiplex histology analysis of thymic tissue (eTable 3); and 10 matched healthy controls from the Münster University Hospital for MIF ELISA analysis.

Tissue Collection and Processing

Thymic samples were dispersed mechanically within 1.5 hours of removal.^{5-7,16} The resulting cell suspensions were then washed and frozen within further 6 hours.⁵ In brief, thymic cells were frozen in 5% dimethyl sulfoxide/95% fetal calf serum at 100–250 × 10⁶ cells in vials held in methanol that was cooled at 5°C per min and subsequently stored over liquid

nitrogen. On thawing, they were diluted by doubling the volume every 45 seconds with Roswell Park Memorial Institute medium (RPMI) plus staphylococcal nuclease (to prevent trapping of viable cells in clumps of congealed DNA) and immediately washed. All samples were carefully thawed and processed in parallel. As expected, we recovered approximately 40% of the input cells.

Flow Cytometry Analysis

Single thymic cell suspensions were stained for 20 minutes at 4°C. After washing, all samples were analyzed using a CytoFLEX flow cytometer (Beckman Coulter, Brea, CA) and FlowJo™ Software V10.8.1; the gating strategy is shown in eFigure 1. The antibodies used were purchased from Biolegend, CD4 (SK3; #344606), CD8 (SK1; #344722), and CD45 (2D1; #368508), and from Becton, Dickinson and Company (BD) Bioscience, CD3 (UCHT1; #557943) and CD19 (SJ25C1; #562653).

Magnetic-Activated Cell Sorting for Single-Cell RNA Sequencing

We enriched CD45⁺ cells using CD45 (tumor-infiltrating lymphocytes) microbeads (Miltenyi Biotec., 130-118-780) according to the manufacturer's protocol. We checked cell numbers and viabilities before and afterward to check for significant cell death.

Generation of Single-Cell Libraries, Next-Generation Sequencing, and Preprocessing of Sequencing Data

CD45⁺ magnetic-activated cell sorting-enriched single-cell suspensions were loaded onto the Chromium Single Cell Controller using the Chromium Next Gel Bead-in-Emulsion (GEM) Single Cell 5' Library and Gel Bead Kit v1.1 chemistry (10x Genomics). The derived barcoded complementary DNA was partly used in Chromium Single Cell V(D)J Enrichment Kits (10x Genomics) for further scBCR-seq. We processed samples and libraries according to the manufacturer's instructions using solid phase reversible immobilization select beads (Beckman Coulter). Sequencing was performed on a local Illumina Nextseq 2000 using the P3 Reagents 100-Cycle Kit with a 26-8-0-91 read setup. One of the samples was then excluded because of the low quality of the data recovered (MG07, eTable 1). We processed sequenced data with the *cellranger* pipeline v.6.1.1 (10X Genomics) according to the manufacturer's instructions. *CellBender* software was applied to remove the counts because of ambient RNA molecules and random barcode swapping from the count matrices.

Data Analysis of scRNA-Seq

Downstream analysis was performed with the R package Seurat v.4.2.0¹⁷ using R v.4.2.1. Only genes present in more than 3 cells and cells with more than 500 genes were retained. Low-quality cells and cell doublets were removed by filtering based on gene count (<500 or >3,000) and high mitochondrial percentages (>10%). After quality control, a total of 33,613 cells remained for further analyses including data normalization, scaling, and principal component analysis (PCA) where cell-cycle gene sets defined in a previous study¹⁸ were removed from the list of variable genes to exclude cell cycle-associated variation and clustering. We removed 2 clusters from the data set that expressed mainly ribosomal genes and most likely represented low-quality cells (11.68% of the cells). Cluster cell identity was assigned by manual annotation using known marker genes and by applying anchor-based label transfer, implemented in Seurat, using as reference a thymic dataset.¹⁸ To achieve a high-resolution annotation in the B lineage, subclustering was performed and batch effects were removed using Harmony.¹⁹ Because B-cell types are so rare in the healthy thymus, the annotation was performed using the anchor-based label transfer Azimuth taking as a reference the tonsil data set.²⁰ Finally, pathway enrichment was conducted using ReactomeGSA.²¹

RNA Velocity and Pseudotime

Spliced/unspliced counts were generated with velocity v0.17.²² We used the run10x pipeline with the cellranger output, the cellranger gene annotation file, and the human repeat masker file from the University of California, Santa Cruz (UCSC) Genome Browser. The resulting loom files were imported into Seurat with the ReadVelocity wrapper. The spliced/unspliced assays were added to the existing Seurat object. We extracted B-lineage cell clusters from the data set and re-ran the Seurat pipeline. Further downstream analysis was performed with scVelo v.0.25²³ according to the official tutorial. The data were preprocessed by normalization, log transformation (top 2,000 genes), PCA, neighborhood graph, and moments estimation. We then used the dynamical model from scVelo to estimate the RNA velocities. Pseudotime analysis was performed using slingshot v2.6 with default parameters, with the naïve B-cell cluster defined as the starting cluster.

Single-Cell Immune Repertoire Analysis

Single-cell B cell receptor (BCR) data were analyzed using scRepertoire following the official vignette.²⁴ The Ig heavy and light chain sequences were combined, and those cells missing 1 or with more than two of the immune receptor chains were excluded. scBCR data were merged with the scRNA-seq object containing the B-lineage cell clusters. BCR clonotypes were classified using the combinations of variable–diversity–joining (VDJ) genes and their CDR3 nucleotide sequences. Relative antibody subclass frequency analyses were performed with Alakazam.²⁵

Inference of Cellular Interactions

We analyzed cellular communications with CellChat.²⁶ Processed and clustered scRNA-seq data from thymic samples were used as an input. We used a truncated mean of 0.1; cell-cell communications expressed by less than 10 cells were removed. The resulting ligand-receptor pairs are based on the CellChat repository.

Multiplex Histology

Characteristics of the 3 donors are presented in eTable 3 (ethical approval EA1/391/16). Their thymic structural pathology was checked by a board-certified neuropathologist, excluding infarcts, abscesses, and hemorrhages. Tissue preparation and multiplex microscopy image acquisition were performed as previously published.^{27,28} Thymus samples were subjected to multiplexed immunofluorescence histology using the antibodies listed in eTables 4 and 5, stained in the indicated order. Images contain 2048 × 2048 pixels and are generated using an inverted wide-field fluorescence microscope with a ×20 objective, a lateral resolution of 325 nm, and an axial resolution above 5 μm. The fluorescence images were subsequently analyzed using Fiji. All used antibodies were validated in human tonsil or lymphnode tissue control tissue.

Macrophage Migration Inhibitory Factor ELISA

Plasma macrophage migration inhibitory factor (MIF) levels (eTable 1) were determined using the human MIF Quantikine ELISA kit (DMF00B, R&D systems) according to the manufacturer's instructions. Serum MIF levels (eTable 2) were assayed with ELISA kits (ProteinTech Group) according to the manufacturer's instructions. The concentration was determined according to the standard curve.

Statistical Analysis

We checked for correlations between different cell type frequencies and between severity scores and MIF expression levels in serum by calculating the Spearman correlation coefficient (R). The Mann-Whitney test was performed on the plasma MIF ELISA results using GraphPad Prism 10. A *p* value < 0.05 was considered statistically significant.

Standard Protocol Approvals, Registrations, and Patient Consents

The study was conducted according to the Declaration of Helsinki and approved by the Ethics Committees of the Universities of Münster (registration nos. 2010-262-f-S, 2011-665-f-S, 2013-350-f-S, 2014-068-f-S, and 2016-053-f-S) and Charité-Universitätsmedizin Berlin (EA1/281/10), London, and Oxford; written informed consents were given by all participants.

Data Availability

Single-cell RNA-seq data have been deposited in the Gene Expression Omnibus repository under reference number GSE233180 and are publicly available as of the date of publication. This article does not report original code. Any

additional information is available from the lead contact on request.

Results

Single-Cell Transcriptome Profiling of EOMG Thymi

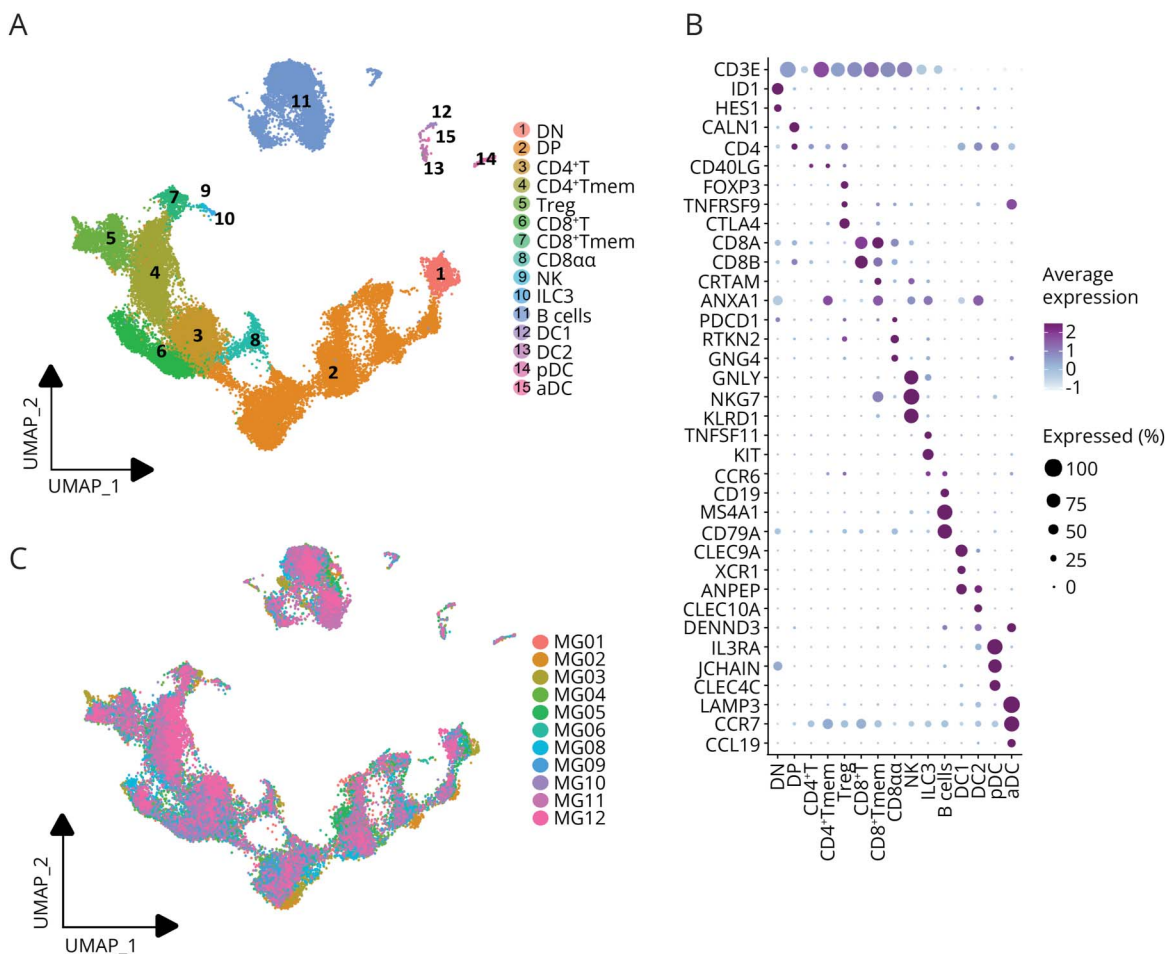
To characterize the immune cellular landscape in EOMG thymi, we first performed scRNA-seq analysis in cryopreserved thymic cell suspensions derived from 11 immunotherapy-naïve patients with AChR-Ab⁺ EOMG with a representative range of demographics (eTable 1). After enrichment for CD45⁺ hematopoietic cells, we profiled 29,688 individual cells and annotated 15 distinct populations (Figure 1A), defined by their expression of cell type-specific transcripts (Figure 1B) and alignment with a reference data set.¹⁸ Each population was represented in each patient, with broadly overlapping distributions and no obvious outliers (Figure 1C).

As expected, T cells were most abundant in each thymic sample. Substantial numbers of B-lineage cells were found in all patients except MG01 (Figure 2A), constituting >5% of the total TFH hematopoietic cells (Figure 2, A–D). This is around 10-fold higher than the previously reported values (0.1%–0.5%) for B cells in non-EOMG thymi.^{29,30}

The EOMG thymic leukocytes contained 8 different T-lineage cell clusters (numbered in Figure 1A): (1) double CD4[−]CD8[−] T-cell precursors, (2) double-positive T cells, (3) single CD4⁺ T cells, (4) CD4⁺ T memory cells, (5) T regulatory cells, (6) CD8⁺ T cells, (7) CD8⁺ T memory cells, and (8) CD8αα⁺. Non-T-cell and non-B-cell populations present in EOMG thymi included natural killer cells, type 3 innate lymphoid cells, and dendritic cells (DCs) including conventional DC1 and DC2 subsets and plasmacytoid DCs.

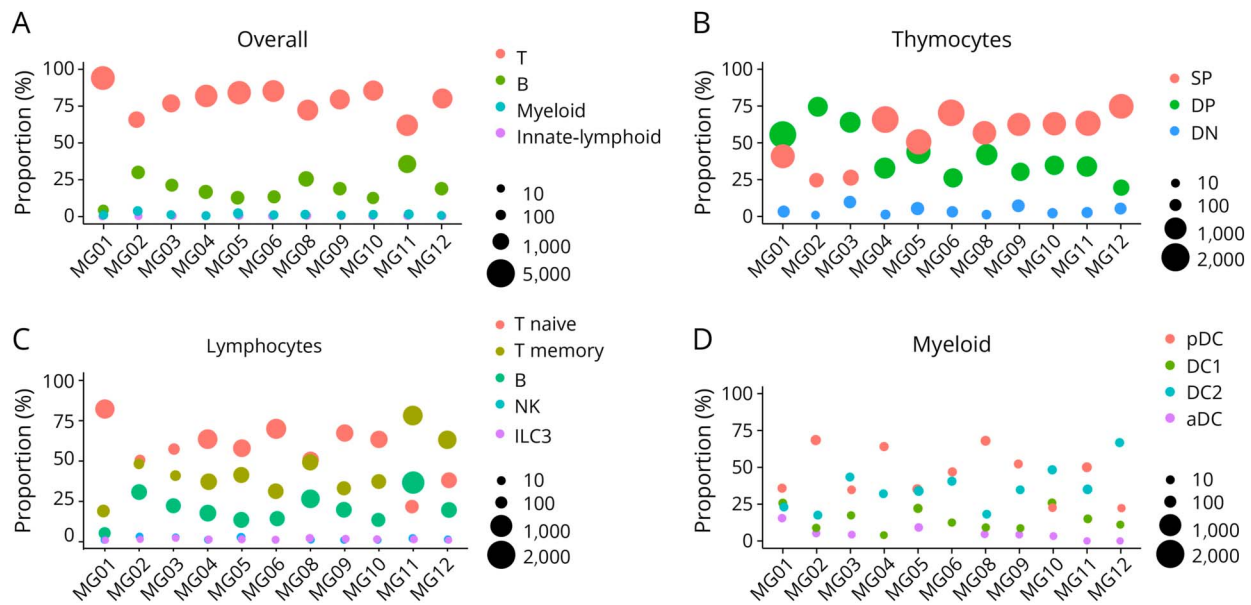
The lymphocyte frequencies from scRNA-seq correlated strongly with those determined by flow cytometry (eFigure 2,

Figure 1 Cellular Landscape and Transcriptional Profile of Lymphoid Cell Types in EOMG Thymi



(A) UMAP visualization of the overall composition of 15 cell types in the pooled data (DN, CD4[−]/CD8[−] double-negative T-cell precursors; DP, double-positive T cells; Treg, T regulatory cells; NK, natural killer cells; ILC3, type 3 innate lymphoid cells; aDC, activated dendritic cells; pDC, plasmacytoid dendritic cells). (B) Dot plot for their expression of selected marker genes in thymic cell types. Here and in later figures, dot color intensities represent average mRNA expression levels within cell types; their sizes indicate the proportions of cells expressing each marker. (C) Same UMAP plot as in A indicating each sample in a different color. EOMG = early-onset AChR-Ab⁺ MG. UMAP = uniform manifold approximation and projection.

Figure 2 Cellular Distribution in EOMG Thymi



Relative proportions of (A) overall cell types, (B) thymocytes, (C) lymphocytes, and (D) myeloid cells in each patient determined by scRNA-seq. Dot sizes represent the absolute cell numbers in the data set. The x axis shows the different patients. EOMG = early-onset AChR-Ab⁺ MG.

A–C). Frequencies of B cells determined by scRNA-seq among lymphocytes correlated positively with plasma anti-AChR titers ($r_s = 0.66$, $p = 0.027$; eFigure 2D).

B-Lineage Subsets in EOMG Thymi

We identified 6 distinct subpopulations of B cells as defined by their transcript combinations (Figure 3, A and C), and comparison was made with a reference data set including tonsils as a control for the lymph node-like infiltrates.²⁰ Each subpopulation was observed in each patient (Figure 3B); the most abundant were (1) memory cells (CD44, KLF2, TNFRSF13B), followed by (2) naïve B cells (FCER2, FCMR, SELL), (3) plasmablasts/plasma cells ([PCs]: JCHAIN, PRDM1, XBP1, MZB1), (4) GC B cells (CD27, CD38, BCL6), and (5) a cycling population expressing cell cycle and proliferation genes (absence of BCL6 and expression of HMGB2, TUBA1B, MKI67, UBE2C). Cycling B cells are separate in their own cluster at higher dimensions because their profile is dominated by these general cycling-specific genes, but they cluster with GC B cells at lower dimensional analysis, likely because of shared proliferation-related gene expression. We also identified (6) a distinct cluster of activated B cells (CD69, MYC), which expressed features of naïve (FCER2), memory (CD44 and TNFRSF13B), and pre-GC stages (MIR155HG) (Figure 3C).

To profile the proliferative capacity of thymic B-lineage cells, we performed a comparative reactome analysis of pathways indicative of cell proliferation and apoptosis (Figure 3D). Apoptosis-related transcripts were enriched in GC, memory, and activated B cells relative to other B-lineage subsets. As expected, cell cycle-related transcripts were much more

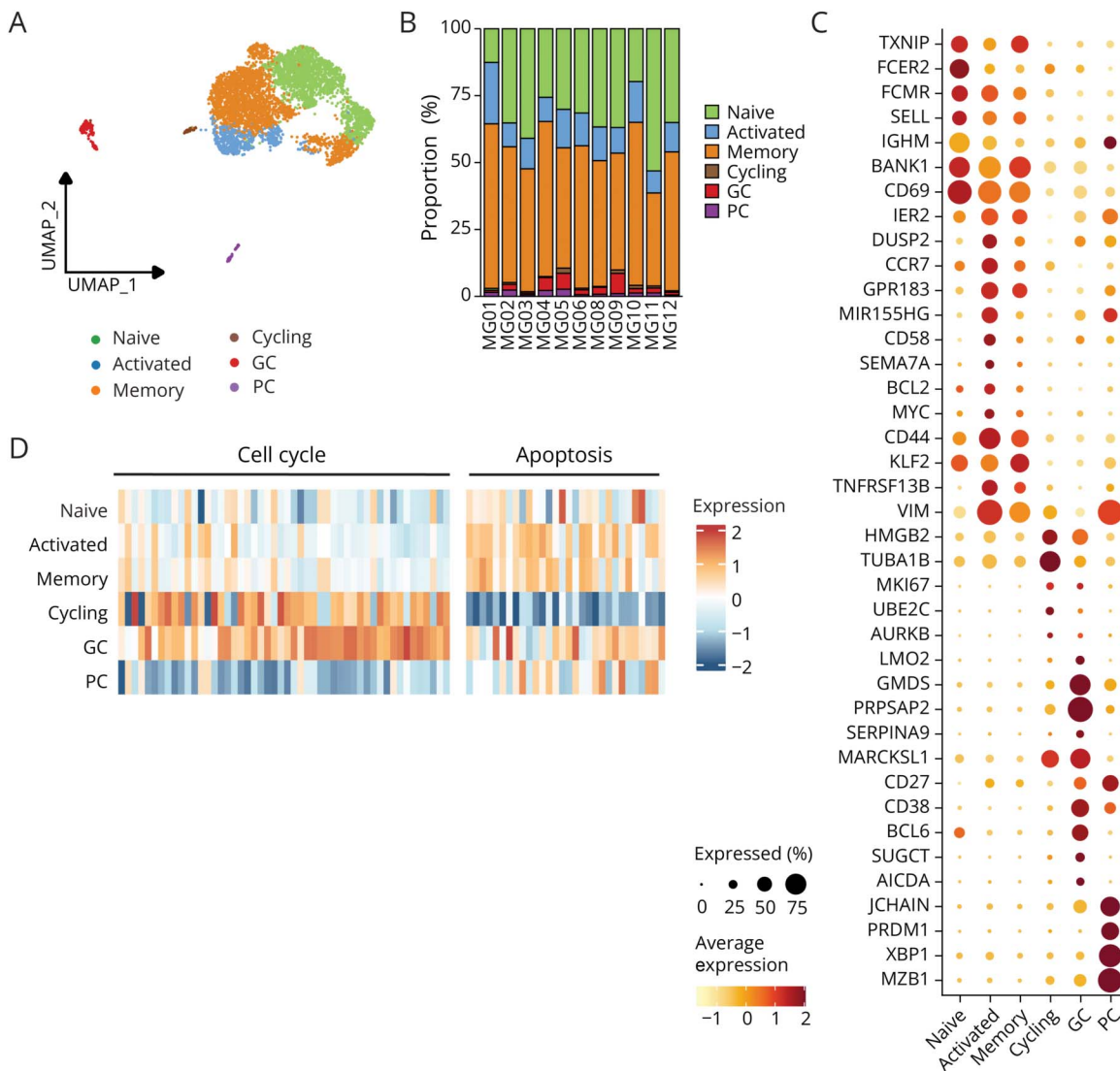
prominent in the cycling and GC B cells than in the naïve, memory, and activated B cells and, especially, the PCs (Figure 3D).

Development of B-Lineage Cell Trajectories in EOMG Thymi

To assess directionality and developmental relationships within the B-cell lineage, we performed RNA velocity and slingshot pseudotime analyses (Figure 4, A–C) and identified 2 developmental trajectories: (1) one starting from naïve going through memory and activated B cells to GC cells (Figure 4B); (2) an additional trajectory going from naïve through activated and cycling B cells and culminating in PCs (Figure 4C). The activated cluster, expressing features from naïve, memory, and pre-GC cells, occupied an intermediate position in both trajectories (Figure 4, B and C). GC cells and PCs have diverged significantly, as they acquire unique traits such as activation-induced cytidine deaminase (AID)/somatic hypermutation and terminal differentiation. The low number of cells in their clusters suggests that early intermediate stages may have been missed. Thus, our analyses highlight distinct transcriptional signatures but may under-represent intermediate states, which could be less apparent due to uniform manifold approximation and projection (UMAP)'s data organization.

We next used single-cell B-cell receptor (scBCR)-seq combined with the scRNA-seq to assess the BCR repertoire of EOMG thymic B-lineage cells and identified 4,536 cells with matching BCR information (eFigure 3). Clonally expanded sequences were most enriched in the GC and cycling B-cell subsets (Figure 4D, eFigure 4A). GCs are critical for the

Figure 3 B-Lineage Subset Distributions in EOMG Thymi



(A) UMAP visualization (GC, germinal center B cells; PC, plasmablasts/plasma cells). (B) Proportions of B-lineage cell subsets in each sample. The x axis shows the different patients. (C) Dot plot showing marker gene expression for the B-lineage cell subsets. (D) Heatmap showing their relative expression levels of key pathways involved in the cell cycle and apoptosis across the different B-cell subsets identified. Each row represents a B-lineage subset and each column a specific pathway. Color intensities indicate relative pathway activities. EOMG = early-onset AChR-Ab⁺ MG; UMAP = uniform manifold approximation and projection.

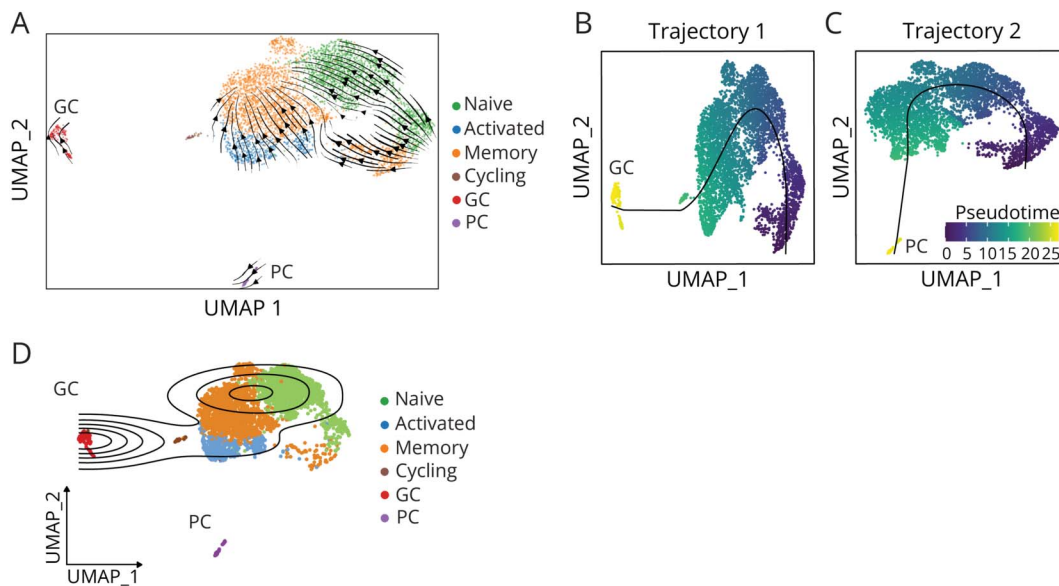
formation of long-lived plasma cells and memory B cells. Within these structures, mature B cells undergo somatic hypermutation (SHM), Ig class switch DNA recombination (CSR), and clonal selection to optimize antigen recognition. Activation-induced cytidine deaminase, encoded by the human activation-induced cytidine deaminase gene (AICDA), is critical for SHM, CSR, and the maturation of Ab responses to foreign and self-antigens. Hence, AICDA-related transcripts were abundantly expressed and enriched in the thymic GC cluster (eFigure 4B). CSR-related proteins and transcripts were predominantly observed in GC and cycling B cells, which exhibited a pre-GC phenotype (eFigure 4B). Analysis of scVDJ-derived antibody class and subclass frequencies across the B lineage identified IgG1 as the most frequently

observed immunoglobulin produced by class-switched EOMG thymic B-lineage cells, followed by IgA1, IgG2, and IgG3 (eFigure 4C). IgA⁺ PCs were also prominent in a previous study on EOMG thymi.⁷

Profiling B-Lineage Cell Interactions in EOMG Thymi

To profile cell-cell communications in EOMG thymi, we integrated single-cell data with a curated ligand-receptor pair database through a bioinformatics application, CellChat (Figure 5A). We included mature T cells and the B-lineage cells in these network analyses. They showed strong interactions between B-lineage cells and T-cell subsets, notably including CD8⁺ T cells (Figure 5, B and C). To better define

Figure 4 B-Lineage Cell Trajectories in EOMG Thymy



(A) Streamline-based visualization of RNA velocity trajectories projected onto the UMAP plot of B-lineage populations from Figure 3A. Streamlines represent directionality, which show their developmental pathways. (B, C) Two lineages of pseudotime analysis of their scRNA-seq populations and pseudotemporal ordering indicated by a color gradient along the trajectories, illustrating their inferred lineage transitions. (D) Contour plot of the distribution of clonally expanded cells on the UMAP embedding. High-density regions in the contour plot indicate areas where clonally expanded cells are concentrated. EOMG = early-onset AChR-Ab⁺ MG; UMAP = uniform manifold approximation and projection.

which signals might support or sustain B-lineage cells, we profiled individual ligand↔receptor interactions from T-cell to B-cell subsets and identified 21 significant pairs, all of them functionally associated with immune cell migration and signaling (Figure 5C).

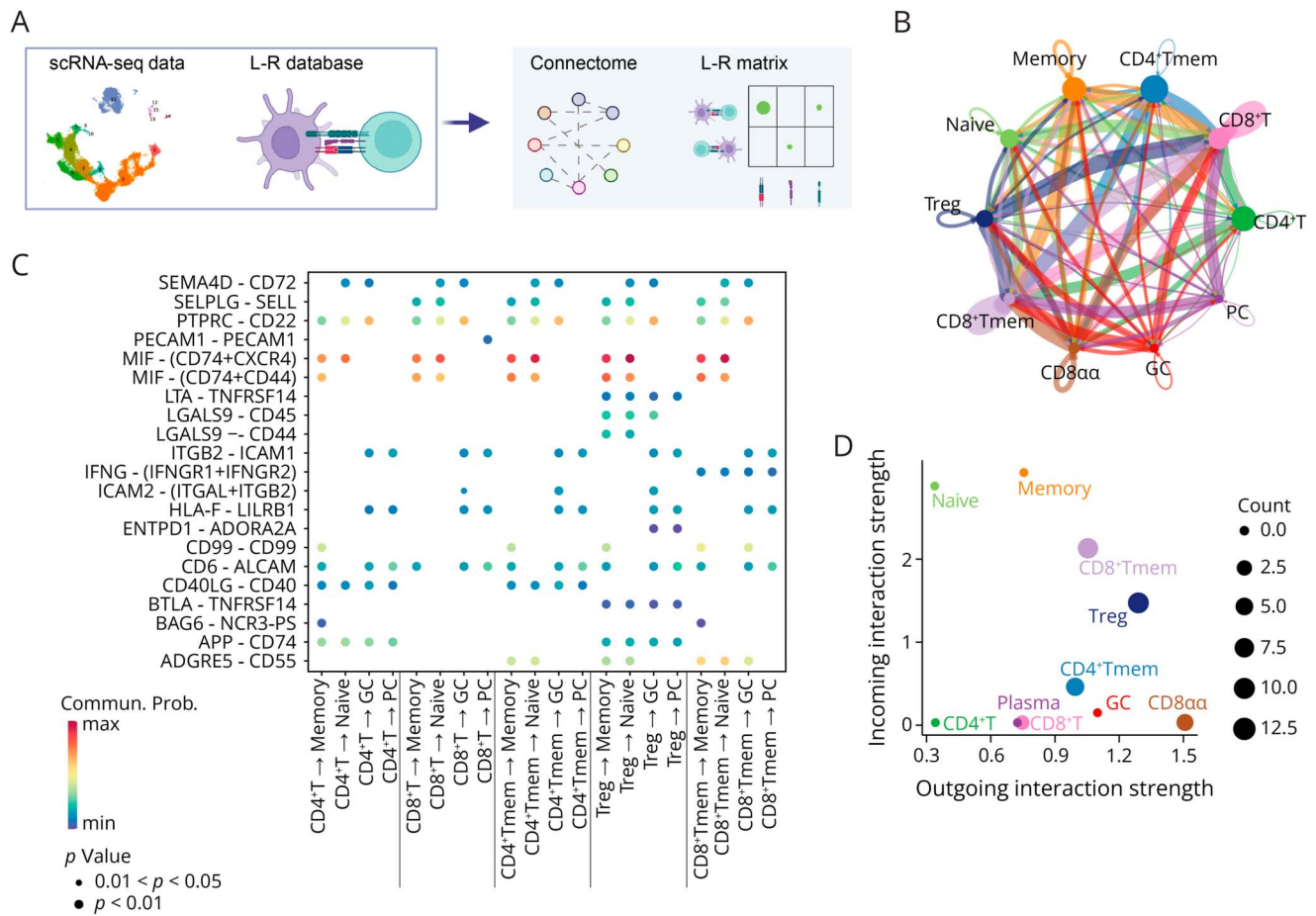
The strongest interaction was predicted for macrophage migration inhibitory factor (MIF; Figure 5C), so we next focused on interaction strengths between different cell types. Surprisingly, in these EOMG thymic samples, we observed that CD8⁺ and regulatory T cells displayed the highest levels of outgoing interactions within the MIF pathway, interacting with its receptors and co-receptors CD74, CXCR4, and CD44 on B-lineage cells, in which the interactions were mainly incoming (Figure 5D). However, GC cells and PCs are strongly human leukocyte antigen (HLA)-class II positive, supposed to express CD74, and so are capable of delivering signals by presenting antigens; malignant plasma cells can also express CD74.³¹ Thus, it would make biological sense for GC B cells and plasma B cells to have low incoming interaction strengths when their role is primarily to present antigen (GC B cells) or secrete antibodies (PCs, which have very few surface receptors and are known to receive minimal incoming interactions). This suggests a central role for these cell types in the MIF pathway. CD74, also referred to as invariant chain, is a type II transmembrane protein expressed on antigen-presenting cells, including the thymus,¹⁸ and also B cells, in which it mediates assembly and trafficking of peptide:major histocompatibility complex class II complexes. CD74 further functions as a *survival* receptor on B cells, essential for

transcriptional regulation of genes that control their proliferation, differentiation, and survival.²⁰ To better assess spatial CD74 expression at the protein level, we used multi-epitope ligand cartography in 3 EOMG thymic tissue samples, which confirmed the expected strong and abundant CD74 and CD44 expression on thymic B cells. The CD74⁺ B-cell accumulations were located mainly in the perivascular space but also in the medullary areas. T cells (major source of MIF on gene expression level) were in proximity with B cells (Figure 6, eFigures 5–7). In addition to B cells, there were some cells with myeloid morphology and strong CD74 expression in frequencies as expected from previous studies.³²

MIF is a proinflammatory cytokine mediating activation in addition to survival of B cells through CD74 ligation. Its expression and secretion are also elevated in most solid and hematogenous cancers, and serum levels of soluble MIF are substantially elevated in patients with B cell–driven autoimmune diseases such as systemic lupus erythematosus.³³

Notably, serum MIF levels reportedly correlate with higher Myasthenia Gravis Foundation of America (MGFA) status and disease severity, as also assessed using the quantitative MG disease score (QMG), in patients with generalized MG.³⁴ Because modern assessments of disease severity are not available for the exploratory cohort, we quantified serum MIF levels in an independent cohort of patients with AChR-Ab–positive EOMG. They were all receiving immunotherapies at the time of sampling (eTable 2). In this study, serum MIF levels correlated with higher MGFA status

Figure 5 Cell-Cell Interactome Predictions Identify Strong Interactions Between GC-Associated and Memory B Cells With T Cells, Dominated by the *MIF-CD74* Axis



(A) Overview of the ligand-receptor interaction analyses. (B) Circle plot shows the inferred intercellular relationships between mature T and B-lineage cells. The thickness of each line represents its total interaction strength. (C) Bubble plot of 21 significant predicted ligand-receptor pairs that contribute to the signaling from mature T cells to B-lineage cells. Colors of dots represent the calculated communication probability, and their sizes indicate the *p*-values computed from one-sided permutation tests. (D) Visualization of the principal predicted sources and targets in the macrophage migration inhibitory factor (MIF) pathway. Dot size ("count") is proportional to the number of inferred links (both outgoing and incoming) associated with each cell group. Interaction strength is the computed communication probability.

(Figure 7A) although not with QMG or activities of daily living scores (Figure 7, B and C) assessed at sampling.

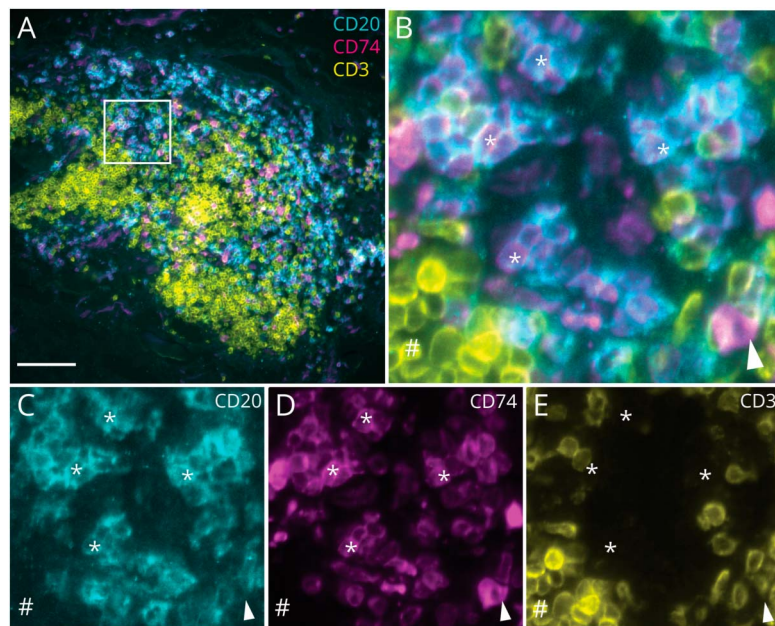
Discussion

Our study demonstrates thymic niches associated with ectopic GC formation and pathologic B-lineage maturation in EOMG, consistent with the clinical benefits of thymectomy and systemic B-cell depletion therapy in EOMG.^{14,15} In healthy controls, the thymus is populated by 2 types of B cells: (1) resident B cells located in the thymic medulla that appear during fetal development and contribute to central T-cell tolerance^{29,30,35} and (2) B cells and PCs that accumulate in thymic perivascular spaces during aging and are predominantly reactive to common antigens encountered through viral infection or vaccination.^{5,7,36} Increased B-cell chemotactic signals and aberrant formation of high endothelial venules are believed to allow for the well-known additional hyperplastic changes in EOMG.³⁷

Our data confirm that the B-lineage cells there differentiate along trajectories similar to those in secondary lymphoid organs and³⁸ exhibit marked functional GC activity—although not always organized identically in other organs³⁹—and features of antigen-driven clonal selection. Our findings thus support the concept that the thymic microarchitecture in EOMG provides activated B-lineage cells with an environment permissive for generating high-affinity and long-lasting autoreactive Ab responses.^{3-7,13}

Regulatory T cells are believed to play an important role in preventing the accumulation of autoreactive clones in the mature naïve B-cell compartment⁴⁰ while cognate interactions of CD4⁺ T helper cells with B cells provide selection signals required for differentiation into GC cells.³⁸ We expected such T-cell help to be crucial for activating autoimmune B cells in EOMG thymi. The absence of T follicular helper (Tfh) cells from our analyses is likely due to their rarity in our samples. Although they play a crucial role in aiding GC

Figure 6 Localization of CD74 in EOMG Thymi by Multiplex Microscopy (MELC)



(A) CD20, CD74, and CD3 are shown in the indicated colors, which are merged. (B) High-power view of the area framed in (A), with single color views in (C), (D), and (E). B cells coexpressing CD20 and CD74 are marked by asterisks (*), a CD74⁺ cell not expressing CD20 is indicated by the arrow (†), and CD3⁺ T cells are marked by the hashtag (#). In (A) scale bar: 100 μ m. EOMG = early-onset AChR-Ab⁺ MG.

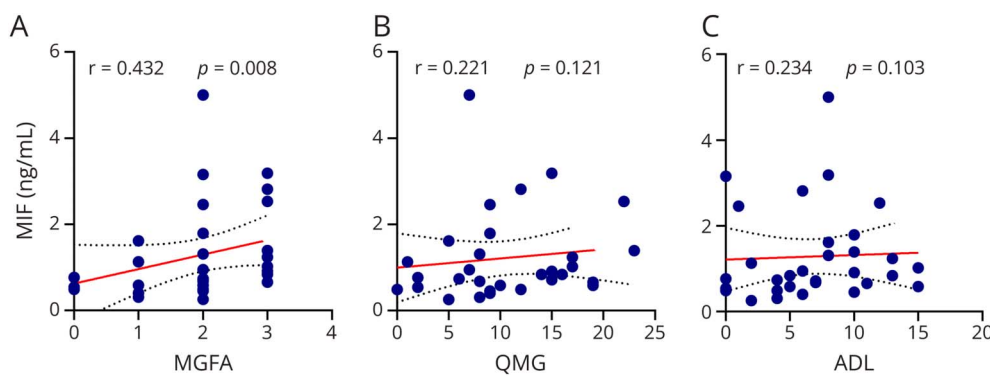
B-cell maturation, they are known to be relatively rare and typically act early in immune responses, so they might be more numerous in earlier samples with larger infiltrates.

Nevertheless, CD4⁺ T-cell interactions with B-lineage cells were surprisingly eclipsed in our samples by others with CD8⁺ T cells. Intriguingly, HLA associations in EOMG have consistently been stronger with HLA-B8 in class I than the linked HLA-DR3 in linked class II in many studies (reviewed by Gregersen et al.^{41,2}), which has always been puzzling in this Th-dependent auto-Ab-mediated disease. These strong predicted interactions with B-lineage cells may again implicate CD8⁺ T cells in pathogenesis of EOMG. This supports a previously hypothesized attack on rare thymic myoid cells that express intact AChR, the only cells outside muscle to do

so,¹² fueling nearby GC responses and thus driving diversification of the ensuing auto-Abs to recognize the intact AChR in its native conformation.^{2,5,41}

A better understanding of mechanisms that facilitate maturation and survival of AChR-specific B-lineage cells in EOMG could provide clues on how to deplete them or restrain the ongoing pathogenicity of their responses. In a recent longitudinal study on patients with MG, anti-CD20 therapy with rituximab (RTX) clearly did not eliminate all auto-Ab-producing B-cell clones, characterized by gene expression signatures associated with B-cell and plasma cell survival, despite substantial depletion of total circulating B cells.⁴² In parallel studies using standard RTX protocols, B-lineage cell clonal expansions likewise persisted in IgM antimyelin-

Figure 7 MIF Expression Levels in Serum



Correlations of (A) MGFA, (B) QMG, and (C) ADL severity scores with serum MIF levels in 32 patients with EOMG. EOMG = early-onset myasthenia gravis; MGFA = Myasthenia Gravis Foundation of America; MIF = macrophage migration inhibitory factor; QMG = quantitative myasthenia gravis disease score; ADL = activities of daily living.

associated glycoprotein peripheral neuropathy and pemphigus vulgaris.^{43,44} This might reflect the important survival signal that CD74 provides to B cells⁴⁵; indeed, it was abundantly expressed in the present EOMG thymi, where its predicted interactions with MIF were among the strongest we observed between thymic T and B-lineage cells. In a recent study, circulating MIF was significantly increased in a wide-ranging cohort of 145 patients with different subtypes of MG, including EOMG, especially in patients with generalized as opposed to ocular MG.³⁴ Moreover, levels of MIF correlated with clinical disease severity as determined by the QMG and decreased in remission,³⁴ further implicating it in the pathogenesis or persistence of MG and highlighting its potential as a predictive biomarker in MG. We observed that serum MIF levels correlate with disease severity as assessed by MGFA status. These correlations are, however, not very strong and require validation in larger independent cohorts of patients with MG.

Our study has limitations with its relatively small numbers of typical steroid-naïve patients with EOMG and should be extended. Deeper analysis of BCR and T-cell receptor sequences could unravel clonally expanded specificities of the adaptive immune response in EOMG thymi, but these investigations are beyond the scope of this study. Moreover, the potential of MIF as a biomarker for disease activity and severity in MG subtypes requires further validation in a larger, prospective cohort.

Besides its role in normal B cells, CD74 ligation results in the release of its intracellular domain, which serves as a transcriptional regulator in chronic lymphocytic leukemia (CLL) B cells,⁴⁶ so CD74-targeting therapies are currently being developed for the treatment of B-lineage malignancies (NCT03424603).^{31,47} Notably, autoimmune conditions, even including MG, occur in up to 25% of patients with CLL and CD5⁺ CLL-like circulating B cells have recently been described in patients with AChR-Ab⁺ MG,⁴⁸ hinting at similar events during their pathogenesis. MIF-targeted biologic therapeutics such as milatuzumab (anti-CD74) are further being evaluated in patients with systemic lupus erythematosus (NCT01845740).⁴⁹ It has also been identified as a promising therapeutic target in rheumatoid arthritis,⁵⁰ where it drives inflammation and immune activation, and in conditions such as melanoma and neurodegenerative diseases,^{51,52} where it modulates the tumor microenvironment and neuroinflammation, respectively. Our study indicates that targeted inhibition of B cell-intrinsic CD74 function might also provide a novel avenue for limiting pathogenic B-lineage cell expansion and persistence in EOMG.³⁴

Acknowledgment

The authors thank Kerstin Stein and Dr. Omar Chuquisana, University Hospital Münster, and Ralf Ücker, Charité Universitätsmedizin Berlin, for expert technical assistance, and Professor Jens-Carsten Rückert (Department of Surgery, Charité–Universitätsmedizin Berlin, Berlin, Germany) for his

support in providing thymic tissue. Raphael Raspe (Department of Neuropathology at Charité Universitätsmedizin Berlin) used his experience in fluorescence microscopy to help carry out the revision experiments.

Author Contributions

P. Terroba-Navajas: drafting/revision of the manuscript for content, including medical writing for content; major role in the acquisition of data; analysis or interpretation of data. I-N. Lu: drafting/revision of the manuscript for content, including medical writing for content; major role in the acquisition of data; analysis or interpretation of data. I. Quast: drafting/revision of the manuscript for content, including medical writing for content. M. Heming: drafting/revision of the manuscript for content, including medical writing for content; analysis or interpretation of data. C.W. Keller: major role in the acquisition of data; analysis or interpretation of data. L. Ostendorf: analysis or interpretation of data. A.E. Hauser: analysis or interpretation of data. R. Mothes: analysis or interpretation of data. H. Radbruch: analysis or interpretation of data. F. Stascheit: major role in the acquisition of data. A.G.O. Meisel: major role in the acquisition of data. H. Wiendl: drafting/revision of the manuscript for content, including medical writing for content. G. Meyer Zu Hörste: drafting/revision of the manuscript for content, including medical writing for content. N. Willcox: major role in the acquisition of data. J.D. Lünemann: drafting/revision of the manuscript for content, including medical writing for content; study concept or design.

Study Funding

I. Quast was supported by the National Health and Medical Research Council Australia (Fellowship APP1145136). A.E. Hauser was supported by Deutsche Forschungsgemeinschaft (DFG) HA5354-10/1, HA5354-12/1 and HA5354-13/1. H. Radbruch and A.G.O. Meisel were supported by a grant from the DFG (KFO5023; TP8 and Z). G. Meyer Zu Hörste was supported by grants from the DFG (ME4050/12-1, ME4050/13-1) and by a grant from the Bundesministerium für Bildung und Forschung (BMBF) “Lipid Immune Neuropathy Consortium”. J.D. Lünemann was supported by grants from the DFG (LU 900/3-1, LU 900/4-1, SFB-TR128-A11).

Disclosure

P. Terroba-Navajas, I-N. Lu, I. Quast, and M.O. Heming report no conflicts of interest. C.W. Keller received support for attending meetings and/or travel from Alexion and UCB Pharma. L. Ostendorf received speaker’s honoraria from Gedel Congress Management GmbH. A.E. Hauser and R. Mothes report no conflicts of interest. H. Radbruch received honoraria from Janssen, Novartis, Sanofi and Alexion. F. Stascheit received support for attending meetings and travel from Alexion and argenx and participated in advisory/data safety monitoring boards of Alexion, Argenx and UCB Pharma. A.G.O. Meisel received speaker or consultancy honoraria or financial research support (paid to his institution) from Alexion Pharmaceuticals, argenx, Axunio,

Destin, Grifols, Hormosan Pharma, Janssen, Merck, Octapharma, UCB, and Xcenda. He serves as medical advisory board chairman of the German MG Society. H. Wiendl received speaker honoraria from Alexion, Biogen, Bristol Myers Squibb, Genzyme, Merck, Neurodiem, Novartis, Ology, Roche, TEVA, and WebMD Global. He received honoraria for consulting services from Abbvie, Actelion, Argencx, BD, Bristol Myers Squibb, EMD Serono, Fondazione Cariplo, Gossamer Bio, Idorsia, Immunic, Immunovant, INmune Bio_Syneos Health, Janssen, Merck, NexGen, Novartis, Roche, Sanofi, Swiss Multiple Sclerosis Society, UCB and Worldwide Clinical Trials. His research is supported by the German MG Society. G. Meyer Zu Hörste received research support from Biogen and Merck Germany; he received honoraria from Alexion and LFB Pharma and participated in Data Safety Monitoring and/or Advisory Boards of LFB Pharma, Roche and Immunovant. N. Willcox reports no conflicts of interest. J.D. Lünemann received speaker fees, research support, travel support, and/or served on advisory boards by Abbvie, Alexion, Argencx, Biogen, Merck, Moderna, Novartis, Roche, Sanofi and Takeda, and is member of the medical advisory board of the German MG Society. Go to [Neurology.org/N](https://www.neurology.org/N) for full disclosures.

Publication History

Received by *Neurology: Neuroimmunology & Neuroinflammation* September 3, 2024. Accepted in final form January 15, 2025. Submitted and externally peer reviewed. The handling editor was Marinos C. Dalakas, MD, FAAN.

References

- Gilhus NE, Tzartos S, Evoli A, Palace J, Burns TM, Verschuuren JJGM. Myasthenia gravis. *Nat Rev Dis Primers*. 2019;5(1):30. doi:10.1038/s41572-019-0079-y
- Willcox N, Leite MI, Kadota Y, et al. Autoimmunizing mechanisms in thymoma and thymus. *Ann N Y Acad Sci*. 2008;1132:163-173. doi:10.1196/annals.1405.021
- Berrih-Aknin S, Cohen-Kaminsky S, Lepage V, Neumann D, Bach JF, Fuchs S. T-cell antigenic sites involved in myasthenia gravis: correlations with antibody titre and disease severity. *J Autoimmun*. 1991;4(1):137-153. doi:10.1016/0896-8411(91)90013-3
- Matthews I, Sims G, Ledwidge S, et al. Antibodies to acetylcholine receptor in parous women with myasthenia: evidence for immunization by fetal antigen. *Lab Invest*. 2002;82(10):1407-1417. doi:10.1097/01.lab.0000032379.63784.9c
- Hill ME, Shiono H, Newsom-Davis J, Willcox N. The myasthenia gravis thymus: a rare source of human autoantibody-secreting plasma cells for testing potential therapeutics. *J Neuroimmunol*. 2008;201-202:50-56. doi:10.1016/j.jneuroim.2008.06.027
- Schluep M, Willcox N, Ritter MA, Newsom-Davis J, Larché M, Brown AN. Myasthenia gravis thymus: clinical, histological and culture correlations. *J Autoimmun*. 1988;1(5):445-467. doi:10.1016/0896-8411(88)90067-4
- Thomas JA, Willcox HN, Newsom-Davis J. Immunohistological studies of the thymus in myasthenia gravis. Correlation with clinical state and thymocyte culture responses. *J Neuroimmunol*. 1982;3(4):319-335. doi:10.1016/0165-5728(82)90035-2
- Mollaiean A, Haas C. A tale of autoimmunity: thymoma, thymectomy, and systemic lupus erythematosus. *Clin Rheumatol*. 2020;39(7):2227-2234. doi:10.1007/s10067-020-05061-z
- Ohe R, Yang S, Yamashita D, et al. Pathogenesis of follicular thymic hyperplasia associated with rheumatoid arthritis. *Pathol Int*. 2022;72(4):252-260. doi:10.1111/pin.13212
- Hurtubise B, Frohman EM, Galetta S, et al. MOG antibody-associated disease and thymic hyperplasia: from the National Multiple Sclerosis Society Case Conference proceedings. *Neural Neuroimmunol Neuroinflamm*. 2023;10(2):e200077. doi:10.1212/NXL.000000000200077
- Bogot NR, Quint LE. Imaging of thymic disorders. *Cancer Imaging*. 2005;5(1):139-149. doi:10.1102/1470-7330.2005.0107
- Hohlfeld R, Wekerle H. Reflections on the "intrathymic pathogenesis" of myasthenia gravis. *J Neuroimmunol*. 2008;201-202:21-27. doi:10.1016/j.jneuroim.2008.05.020
- Graus YF, de Baets MH, Parren PW, et al. Human anti-nicotinic acetylcholine receptor recombinant Fab fragments isolated from thymus-derived phage display libraries from myasthenia gravis patients reflect predominant specificities in serum and block the action of pathogenic serum antibodies. *J Immunol*. 1997;158(4):1919-1929. doi:10.4049/jimmunol.158.4.1919
- Wolfe GI, Kaminski HJ, Aban IB, et al. Randomized trial of thymectomy in myasthenia gravis. *N Engl J Med*. 2016;375(6):511-522. doi:10.1056/NEJMoa1602489
- Wolfe GI, Kaminski HJ, Aban IB, et al. Long-term effect of thymectomy plus prednisone versus prednisone alone in patients with non-thymomatous myasthenia gravis: 2-year extension of the MGTX randomised trial. *Lancet Neurol*. 2019;18(3):259-268. doi:10.1016/S1474-4422(18)30392-2
- Kakalacheva K, Maurer MA, Tackenberg B, Münz C, Willcox N, Lünemann JD. Intrathymic Epstein-Barr virus infection is not a prominent feature of myasthenia gravis. *Ann Neurol*. 2011;70(3):508-514. doi:10.1002/ana.22488
- Hao Y, Hao S, Andersen-Nissen E, et al. Integrated analysis of multimodal single-cell data. *Cell*. 2021;184(13):3573-3587.e29. doi:10.1016/j.cell.2021.04.048
- Park JE, Botting RA, Domínguez Conde C, et al. A cell atlas of human thymic development defines T cell repertoire formation. *Science*. 2020;367(6480):eaay3224. doi:10.1126/science.aay3224
- Korsunsky I, Millard N, Fan J, et al. Fast, sensitive and accurate integration of single-cell data with Harmony. *Nat Methods*. 2019;16(12):1289-1296. doi:10.1038/s41592-019-0619-0
- King HW, Orban N, Riches JC, et al. Single-cell analysis of human B cell maturation predicts how antibody class switching shapes selection dynamics. *Sci Immunol*. 2021;6(56):eabe6291. doi:10.1126/sciimmunol.abe6291
- Griss J, Viteri G, Sidiropoulos K, Nguyen V, Fabregat A, Hermjakob H. ReactomeGSA—efficient multi-omics comparative pathway analysis. *Mol Cell Proteomics*. 2020;19(12):2115-2125. doi:10.1074/mcp.TIR120.002155
- La Manno G, Soldatov R, Zeisel A, et al. RNA velocity of single cells. *Nature*. 2018;560(7719):494-498. doi:10.1038/s41586-018-0414-6
- Bergen V, Lange M, Peidli S, Wolf FA, Theis FJ. Generalizing RNA velocity to transient cell states through dynamical modeling. *Nat Biotechnol*. 2020;38(12):1408-1414. doi:10.1038/s41587-020-0591-3
- Borcherding N, Bormann NL, Kraus G. scRepertoire: an R-based toolkit for single-cell immune receptor analysis. *F1000Res*. 2020;9:47. doi:10.12688/f1000res.22139.2
- Gupta NT, Vander Heiden JA, Uduman M, Gadala-Maria D, Yaari G, Kleinstein SH. Change-O: a toolkit for analyzing large-scale B cell immunoglobulin repertoire sequencing data. *Bioinformatics*. 2015;31(20):3356-3358. doi:10.1093/bioinformatics/btv359
- Jin S, Guerrero-Juarez CF, Zhang L, et al. Inference and analysis of cell-cell communication using CellChat. *Nat Commun*. 2021;12(1):1088. doi:10.1038/s41467-021-21246-9
- Holzwarth K, Kohler R, Philipsen L, et al. Multiplexed fluorescence microscopy reveals heterogeneity among stromal cells in mouse bone marrow sections. *Cytometry A*. 2018;93(9):876-888. doi:10.1002/cyto.a.23526
- Pascual-Reguant A, Köhler R, Mothes R, et al. Multiplexed histology analyses for the phenotypic and spatial characterization of human innate lymphoid cells. *Nat Commun*. 2021;12(1):1737. doi:10.1038/s41467-021-21994-8
- Perera J, Meng L, Meng F, Huang H. Autoreactive thymic B cells are efficient antigen-presenting cells of cognate self-antigens for T cell negative selection. *Proc Natl Acad Sci U S A*. 2013;110(42):17011-17016. doi:10.1073/pnas.1313001110
- Frommer F, Heinen TJ, Wunderlich FT, et al. Tolerance without clonal expansion: self-antigen-expressing B cells program self-reactive T cells for future deletion. *J Immunol*. 2008;181(8):5748-5759. doi:10.4049/jimmunol.181.8.5748
- Burton JD, Ely S, Reddy PK, et al. CD74 is expressed by Multiple myeloma and is a promising target for therapy. *Clin Cancer Res*. 2004;10(19):6606-6611. doi:10.1158/1078-0432.CCR-04-0182
- Payet CA, You A, Fayet OM, et al. Central role of macrophages and nucleic acid release in myasthenia gravis thymus. *Ann Neurol*. 2023;93(4):643-654. doi:10.1002/ana.26590
- Mizue Y, Nishihira J, Miyazaki T, et al. Quantitation of macrophage migration inhibitory factor (MIF) using the one-step sandwich enzyme immunosorbent assay: elevated serum MIF concentrations in patients with autoimmune diseases and identification of MIF in erythrocytes. *Int J Mol Med*. 2000;5(4):397-403. doi:10.3892/ijmm.5.4.397
- Huang X, Li H, Zhang Z, Wang Z, Du X, Zhang Y. Macrophage migration inhibitory factor: a novel biomarker upregulates in myasthenia gravis and correlates with disease severity and relapse. *Cytokine*. 2024;175:156485. doi:10.1016/j.cyt.2023.156485
- Afzali AM, Nirschl L, Sie C, et al. B cells orchestrate tolerance to the neuromyelitis optica autoantigen AQP4. *Nature*. 2024;627(8003):407-415. doi:10.1038/s41586-024-07079-8
- Núñez S, Moore C, Gao B, et al. The human thymus perivascular space is a functional niche for viral-specific plasma cells. *Sci Immunol*. 2016;1(6):eaah4447. doi:10.1126/sciimmunol.aah4447
- Weiss JM, Cufi P, Bismuth J, et al. SDF-1/CXCL12 recruits B cells and antigen-presenting cells to the thymus of autoimmune myasthenia gravis patients. *Immunobiology*. 2013;218(3):373-381. doi:10.1016/j.imbio.2012.05.006
- De Silva NS, Klein U. Dynamics of B cells in germinal centres. *Nat Rev Immunol*. 2015;15(3):137-148. doi:10.1038/nri3804
- Hutloff A. T follicular helper-like cells in inflamed non-lymphoid tissues. *Front Immunol*. 2018;9:1707. doi:10.3389/fimmu.2018.01707
- Sng J, Ayoglu B, Chen JW, et al. AIRE expression controls the peripheral selection of autoreactive B cells. *Sci Immunol*. 2019;4(34):eaav6778. doi:10.1126/sciimmunol.aav6778
- Gregersen PK, Kosoy R, Lee AT, et al. Risk for myasthenia gravis maps to a (151) Pro→Ala change in TNIP1 and to human leukocyte antigen-B*08. *Ann Neurol*. 2012;72(6):927-935. doi:10.1002/ana.23691

42. Jiang R, Fichtner ML, Hoehn KB, et al. Single-cell repertoire tracing identifies rituximab-resistant B cells during myasthenia gravis relapses. *JCI Insight*. 2020;5(14):e136471. doi:10.1172/jci.insight.136471
43. Maurer MA, Rakocevic G, Leung CS, et al. Rituximab induces sustained reduction of pathogenic B cells in patients with peripheral nervous system autoimmunity. *J Clin Invest*. 2012;122(4):1393-1402. doi:10.1172/JCI58743
44. Colliou N, Picard D, Caillot F, et al. Long-Term remissions of severe pemphigus after rituximab therapy are associated with prolonged failure of desmoglein B cell response. *Sci Transl Med*. 2013;5(175):175ra30. doi:10.1126/scitranslmed.3005166
45. David K, Friedlander G, Pellegrino B, et al. CD74 as a regulator of transcription in normal B cells. *Cell Rep*. 2022;41(5):111572. doi:10.1016/j.celrep.2022.111572
46. Binsky I, Haran M, Starlets D, et al. IL-8 secreted in a macrophage migration-inhibitory factor- and CD74-dependent manner regulates B cell chronic lymphocytic leukemia survival. *Proc Natl Acad Sci U S A*. 2007;104(33):13408-13413. doi:10.1073/pnas.0701553104
47. Chan WK, Williams J, Sorathia K, et al. A novel CAR-T cell product targeting CD74 is an effective therapeutic approach in preclinical mantle cell lymphoma models. *Exp Hematol Oncol*. 2023;12(1):79. doi:10.1186/s40164-023-00437-8
48. Ingelfinger F, Kramer M, Lutz M, et al. Antibodies produced by CLL phenotype B cells in patients with myasthenia gravis are not directed against neuromuscular endplates. *Neurol Neuroimmunol Neuroinflamm*. 2023;10(2):e200087. doi:10.1212/nxi.000000000200087
49. Wallace DJ, Figueras F, Wegener WA, Goldenberg DM. Experience with milatuzumab, an anti-CD74 antibody against immunomodulatory macrophage migration inhibitory factor (MIF) receptor, for systemic lupus erythematosus (SLE). *Ann Rheum Dis*. 2021;80(7):954-955. doi:10.1136/annrheumdis-2020-219803
50. Leech M, Lacey D, Xue JR, et al. Regulation of p53 by macrophage migration inhibitory factor in inflammatory arthritis. *Arthritis Rheum*. 2003;48(7):1881-1889. doi:10.1002/art.11165
51. de Azevedo RA, Shoshan E, Whang S, et al. MIF inhibition as a strategy for overcoming resistance to immune checkpoint blockade therapy in melanoma. *Oncimmunology*. 2020;9(1):1846915. doi:10.1080/2162402X.2020.1846915
52. Zeng L, Hu P, Zhang Y, et al. Macrophage migration inhibitor factor (MIF): potential role in cognitive impairment disorders. *Cytokine Growth Factor Rev*. 2024;77:67-75. doi:10.1016/j.cytogfr.2024.03.003